HHS Public Access

Author manuscript

*Clin Cancer Res*. Author manuscript; available in PMC 2017 February 15.

Published in final edited form as:

*Clin Cancer Res*. 2016 February 15; 22(4): 1000–1010. doi:10.1158/1078-0432.CCR-14-3156.

# Effect of a Smac Mimetic (TL32711, Birinapant) on the Apoptotic Program and Apoptosis Biomarkers Examined with Validated Multiplex Immunoassays Fit for Clinical Use

**Apurva K. Srivastava**[1], **Soumya Jaganathan**[1], **Laurie Stephen**[2], **Melinda G. Hollingshead**[3], **Adam Layhee**[2], **Eric Damour**[2], **Jeevan Prasaad Govindharajulu**[1], **Jennifer Donohue**[2], **Dominic Esposito**[4], **James P. Mapes**[2], **Robert J. Kinders**[1], **Naoko Takebe**[5], **Joseph E. Tomaszewski**[6], **Shivaani Kummar**[6], **James H. Doroshow**[6], and **Ralph E. Parchment**[1]

[1]Laboratory of Human Toxicology and Pharmacology, Applied/Developmental Research Directorate, Leidos Biomedical Research, Inc., Frederick National Laboratory for Cancer Research, Frederick, Maryland, 21702

[2]Myriad RBM, Austin, Texas, 78759

[3]Biological Testing Branch, Developmental Therapeutics Program, Frederick National Laboratory for Cancer Research, Frederick, Maryland, 21702

[4]Protein Expression Laboratory, Cancer Research Technology Program, Leidos Biomedical Research, Inc., Frederick National Laboratory for Cancer Research, Frederick, Maryland, 21702

[5]Investigational Drug Branch, Division of Cancer Treatment and Diagnosis, National Cancer Institute, Bethesda, MD, 20892

[6]Division of Cancer Treatment and Diagnosis, National Cancer Institute, Bethesda, MD, 20892

## Abstract

**Purpose—**To support clinical pharmacodynamic evaluation of the Smac mimetic TL32711 (birinapant) and other apoptosis-targeting drugs, we describe the development, validation, and application of novel immunoassays for 15 cytosolic and membrane-associated proteins indicative of the induction, onset, and commitment to apoptosis in human tumors.

**Experimental Design—**The multiplex immunoassays were constructed on the Luminex platform with apoptosis biomarkers grouped into three panels. Panel 1 contains Bak, Bax, total caspase-3, total lamin-B (intact and 45 kDa fragment), and Smac; panel 2 contains Bad, Bax–Bcl-2 heterodimer, Bcl-xL, Bim, and Mcl1; and panel 3 contains active (cleaved) caspase-3, Bcl-xL–Bak heterodimer, Mcl1–Bak heterodimer, pS99-Bad, and survivin. Antibody specificity was confirmed by immunoprecipitation and Western analysis.

Corresponding Author: Apurva K. Srivastava, Laboratory of Human Toxicology and Pharmacology, Applied/Developmental Research Directorate, Leidos Biomedical Research, Inc., Frederick National Laboratory of Cancer Research, PO Box B, Frederick, MD 21702. Phone: (301) 846-6096; Fax: (301) 846-6536; srivastavaa4@mail.nih.gov.

**Disclosure of Potential Conflicts of Interest:** L.S., A.L., E.D., and J.P.M. are employed by Myriad RBM, which has a commercial interest in the product described in this manuscript.

**Results—**Two laboratories analytically validated the multiplex immunoassays for application with core needle biopsy samples processed to control pre-analytical variables; the biological variability for each biomarker was estimated from xenograft measurements. Studies of TL32711 in xenograft models confirmed a dose-dependent increase in activated caspase-3 6 hours after dosing and provided assay fit-for-purpose confirmation. Coincident changes in cytosolic lamin-B and subsequent changes in Bcl-xL provided correlative evidence of caspase-3 activation. The validated assay is suitable for use with clinical specimens; 14 of 15 biomarkers were quantifiable in patient core needle biopsies.

**Conclusions—**The validated multiplex immunoassays developed for this study provided proof of mechanism data for TL32711 and are suitable for quantifying apoptotic biomarkers in clinical trials.

### Keywords

Apoptosis; pharmacodynamic assay; birinapant; multiplex immunoassays; Smac mimetic

## INTRODUCTION

Overexpression of pro-survival proteins in cancer cells often shifts the equilibrium between pro-apoptotic and pro-survival proteins in favor of cell survival (1, 2); considerable effort is therefore being directed toward developing novel therapeutic agents that target apoptotic control points in tumor cells (3–9). One critical limitation for the clinical characterization of such agents is the absence of assays capable of measuring targeted effects in tumor tissue. To date, measurable pharmacodynamic (PD) biomarkers of target engagement and action in the apoptotic pathway have been limited to a few circulating fragments of proteins generated during apoptosis, such as cytokeratin 18, that provide indirect measurements of drug effect with no indication that the biomarker originated from the tumor (10). Immunohistochemical determination of Ki67 and cleaved caspases are the most studied PD biomarkers of drug-induced apoptosis in tumor samples (11, 12). Immunoprecipitation (IP) and immunoblotting (WB) assays for apoptosis pathway proteins have also been used to demonstrate drug effects and can measure critical heterodimeric proteins that control apoptosis; however, protein acquired from 18-gauge needle biopsies is insufficient to make the IP approach feasible in the clinical trial setting (13, 14). Assays capable of quantifying drug effect directly on biomarkers indicating induction, onset, and commitment to apoptosis in clinically relevant tumor biopsy samples would enhance the evaluation of new drugs.

Apoptosis is a tightly regulated, multi-step process involving extrinsic (receptor) and intrinsic (mitochondrial) pathways (15, 16). Intrinsic apoptosis is regulated by the Inhibitors of Apoptosis (IAP) and Bcl-2 protein families, some of which promote cell survival while others promote cell death (17–21). A subset of the Bcl-2 family proteins, including Bad, Bid, Bim, p53 up-regulated modulator of apoptosis (Puma), and phorbol-12-myristate-13-acetate-induced protein 1 (Noxa), are involved in sensing stress signals in the cell. When triggered, these sensor proteins mediate the activation of pro-apoptotic effector proteins such as Bax and Bak. The effector proteins insert into the outer mitochondrial membrane and homo- or hetero-oligomerize to form pores and release caspase-activating factors such as cytochrome-c and second mitochondrial activator of caspases (Smac) into the cytosol. Smac,

in turn, binds to IAPs such as cellular IAP1/2 (cIAP1/2), X chromosome-linked IAP (XIAP), and survivin, to deactivate the IAPs and favor caspase activation. Under normal cellular conditions, pro-apoptotic proteins are kept in check by heterodimerization with pro-survival members of the Bcl-2 family, such as Bcl-2, Bcl-xL, Bcl-w, Mcl1, and Bcl-2-related protein A1 (Bfl-1/A1).

Cancer therapeutics targeting the intrinsic apoptosis pathway attempt to alter the balance of Bcl-2 family oligomers to trigger apoptosis (18, 20, 22–24). TL32711 (birinapant) is a biindole-based bivalent Smac mimetic that promotes apoptosis by mimicking the binding of Smac to cIAP1/2 and XIAP, deactivating their caspase inhibition (5, 7, 25, 26). This agent is currently in phase 2 trials, and early reports indicate on-target activity (27). To provide greater insight into the PD effects of TL32711, and potentially other drugs targeting the programmed cell death pathway, we describe here the development of multiplex immunoassays measuring 15 potential PD biomarkers found in the cytosolic and nuclear/membrane fractions of tumor biopsy extracts indicating induction, onset, and commitment to apoptosis. We employed multiplexed sandwich immunoassays to quantitate both monomeric and heterodimeric forms of Bcl-2 family proteins in tumor lysates, a novel approach that evaluates the pathway based on alterations in protein interactions and dynamics rather than absolute protein levels. Observed changes in caspase-3 activation and the subsequent degradation of lamin-B and Bcl-xL in xenograft tumor biopsies demonstrated TL32711 drug action and assay fitness-for-purpose. Finally, we established the feasibility of measuring potential PD effects in early phase clinical trials by testing needle biopsy specimens from several patients with solid tumors to establish baseline expression levels of these 15 members of the apoptotic pathway.

## MATERIAL AND METHODS

### Antibodies, recombinant calibrators, and linked heterodimer fusion proteins

Antibodies and several calibrator proteins were purchased from commercial sources (R&D Systems, Santa Cruz Biotechnology, Trevigen, Abcam, Thermo Scientific, Epitomics, Inc., Origene, Enzo, and Proteintech). Antibody preparations free from carrier proteins and stabilizers were conjugated to biotin using Sulfo-NHS-LC-Biotin (Thermo Scientific, Pierce EZ-Link) according to manufacturer's recommended procedures employing a 25:1 biotin:antibody ratio (Supplemental Data). Recombinant protein calibrators lamin-B, Mcl-1, Bcl-xL, survivin, intact caspase-3, active (cleaved) caspase-3, Bax, Bak, Bad, and Bim were obtained commercially, while Smac, pS99-Bad, and all heterodimers (Bcl-xL–Bak, Mcl1–Bak, and Bax–Bcl-2) were designed at the Protein Expression Laboratory (Leidos Biomedical Research, Inc., Frederick National Laboratory for Cancer Research). Recombinant protein calibrator concentrations were based on BCA protein measurements.

Linked heterodimer fusion protein constructs used the Bcl-xL amino acids (aa) 2-85, Mcl1 aa 2-300, Bak aa 2-185, and Bax aa 2-187 as appropriate, and included a 20 aa linker composed of Gly, Ala, and Ser (GSGAGGSAGGSGAGSGAGSG) between the two proteins in each heterodimer. Variable linker lengths were tested; the 20 aa linker allowed free formation of the proper multimeric structure while constraining the two proteins in a single molecule and providing maximum structural flexibility. Proteins were expressed in either

insect SF5 or HEK293 mammalian cells using the baculovirus expression vector system and purified (Supplemental Data). The presence of individual proteins in the purified heterodimers was confirmed by immunoblotting (data not shown).

### Preparation of fractionated tumor tissue and cell lysates

Pre-chilled (4°C) cytosolic extraction buffer (CEB, Myriad RBM), supplemented with PhosSTOP (Roche) and protease inhibitor tablets (Roche) per manufacturer recommendation, was added to xenograft tissues (350 μL CEB per 5–15 mg wet weight tissue) or cell pellets (350 μL CEB per $1\times10^7$ – $3\times10^7$ cells). Tissues were first minced with fine scissors, then immediately homogenized with a PRO200 homogenizer (PRO Scientific) with Multi-Gen adaptor and 5 mm generator at a medium (3) setting for 5 sec. Samples were placed in an ice/water bath and incubated for 10 minutes. Lysates were centrifuged at 16,000 × *g* for 30 minutes at 4°C. The supernatant (cytoplasmic fraction) was carefully removed without disturbing the pellet (containing the nucleus, membrane and mitochondrial fraction), supplemented with detergents [17.5 μL 20% Triton X-100 (Roche) and 21 μl 10% CHAPS (Sigma)], and stored at −80°C for later analysis. The pellet was washed twice with 350 μL CEB and then resuspended in 350 μL membrane extraction buffer (MEB, Myriad RBM, with PhosSTOP and protease inhibitors) by vortexing and incubated at 4°C for 45 minutes with orbital shaking. After centrifugation at 16,000 × g for 10 minutes at 4°C, the clarified supernatant (mitochondrial/nuclear fraction) was carefully removed and aliquoted for analyses; the pellet was discarded. Total protein levels in both the cytoplasmic and mitochondrial/nuclear fractions were measured by Pierce BCA Protein Assay (Thermo Scientific).

### Luminex bead multiplex immunoassays

The immunoassays were built on the Luminex xMAP multiplex technology platform using magnetic bead capture. Washes were performed with a 96-well magnetic plate washer (ELx405, BioTek). During incubation, the plates were placed on an orbital titer plate shaker (VWR International). Liquid handling was performed manually with calibrated, adjustable, precision multichannel pipettes (Rainin 8-Channel). All assays were performed in 96-well plates (BioPlex, BioRad) at 25°C ± 3°C by adding 10 μL of blocking solution (Myriad RBM) and 30 μL of calibrator, control, or unknown sample. Antibody-coupled beads were sonicated for 5 seconds and then vortexed at medium speed for 10–20 seconds to disperse the beads, and 10 μL beads (250 beads/analyte/μL) were added to each well per analyte. Plates were protected from light (Black Microplate Lid, VWR) and incubated for 1 hour at 25°C ± 3°C with shaking. Plates were washed with wash solution (Myriad RBM), and then 40 μL of detection antibody-biotin conjugate was added and plates were incubated for an additional hour with shaking. After incubation with the antibody-biotin conjugate, 40 μL of R-phycoerythrin–labeled streptavidin (Invitrogen) was added, and plates were incubated for 30 minutes with shaking. After a final wash, 100 μL of assay buffer was added to each well and plates were read on a Luminex 200 reader.

### Analytical validation of the multiplex immunoassays

To determine reproducibility, control specimens were prepared by Myriad RBM using tumor lysates (and spiked with recombinant proteins when necessary for low abundance analytes) to bring analyte concentrations close to the EC20, EC50, and EC80 of the individual calibration curves. The sensitivity or lower limit of quantitation (LLOQ) for each marker was determined by calculating the mean of the blank ± 10 standard deviation (SD) for 20 blank wells (Table 1). The functional limit of detection (F-LOD) was defined as the lowest control sample measurement above LLOQ that resulted in an assay precision <30% CV. The upper limit of quantitation (ULOQ) was set at the highest measured calibrator for each biomarker standard curve.

Analysis of dilution linearity was carried out on high, medium, and low control samples generated by Myriad RBM using PC-3 and MCF-7 xenograft and human colorectal tumor tissue lysates obtained from Proteogenex (spiked with recombinant proteins for low abundance analytes) diluted 1:2, 1:4, and 1:8 with assay diluent; recoveries between 70% and 130% were considered acceptable to demonstrate minimal effect of sample matrix on biomarker measurements. Accuracy was evaluated by spike/recovery of standards for each biomarker in pooled xenograft extracts at four concentrations representing the dynamic range of the assay; data were calculated as the proportion of observed-to-expected standard. Inter-laboratory performance was determined using the high, medium, and low control samples described above prepared independently at each site and adjusted to a final concentration of 250–500 μg/mL. Reproducibility was determined by intra-plate (n=20) and inter-day (n=5) variation measured by multiple operators over a minimum of five different days.

### Specificity of multiplex measurements

To establish whether any single antibody cross-reacted with other calibrator proteins, we measured the signal intensity of each bead using multiplexed beads, a cocktail of all calibrators, and single detection (or reporter) antibodies. If there was a signal from a particular bead region from an unrelated detection antibody, further studies were performed to determine the extent of cross-reactivity. Specificity of capture and detector antibodies was demonstrated by immunoprecipitation and subsequent Western blotting of approximately 500 μg of cell or tissue lysates (Supplemental Data).

### Evaluation of pre-analytical factors

Pre-analytical variables such as stability of extracts at different storage temperatures and freeze-thaw cycles were determined in six different total cell lysates (Supplemental Data).

### Animal models and drug administration

Athymic nude mice (nu/nu NCr; Animal Production Program, National Cancer Institute [NCI] at Frederick) 50 days of age (~18 g) were implanted with human MDA-MB-231 (breast adenocarcinoma), A375 (melanoma), HCT 116 (colorectal carcinoma), HepG2 (hepatocellular carcinoma), Jurkat (T-cell leukemia), MCF-7 (breast adenocarcinoma), OVCAR3 (ovarian adenocarcinoma), SW620 (colorectal adenocarcinoma), and Jurkat (acute T cell leukemia) cell lines by subcutaneous injection as described (28). Mice were

randomized before initiation of treatment using a commercial software program (Study Director, Studylog Systems, Inc.). Cancer cell lines were obtained from the Division of Cancer Treatment & Diagnosis Repository, NCI at Frederick, except for A375, which was purchased from ATCC. All frozen stocks of each cell line were tested and authenticated by DNA short tandem repeat screening using the AmpFLSTR® Identifiler® (Applied Biosystems) methodology and held no more than 20 passages. TL32711 (NSC 756502) was provided by Tetralogic Pharmaceuticals through a material transfer agreement with the Cancer Therapy Evaluation Program, NCI. TL32711 was administered by intraperitoneal injection in vehicle (10% ethanol, 5% Tween 80, 85% dextrose in water).

NCI at Frederick is accredited by the Association for Assessment and Accreditation of Laboratory Animal Care International and follows USPHS Policy for the Care and Use of Laboratory Animals. All the studies were conducted according to an approved animal care and use committee protocol in accordance with the procedures outlined in the “Guide for Care and Use of Laboratory Animals, Eighth Edition” (National Research Council; 2011; National Academy Press; Washington, D.C.).

### Fit-for-purpose validation of the multiplex immunoassays

Female mice bearing MDA-MB-231 or OVCAR3 xenografts were randomized to treatment arms when tumors reached 200 ± 25 $mm^3$ (study day 1) and dosed on study days 1, 4, and 7 with vehicle or TL32711 at either 12 mg/kg or 4 mg/kg per dose (30 mice per treatment group). Tumor quadrants were collected after doses 1 and 3 (29), fractionated, and stored at −80°C until analysis. For evaluation of efficacy, tumor volumes were recorded after dosing on study days 1, 4, and 7.

### Patient tumor sample collection

Needle biopsies were collected from patients with various types of solid tumors at the NIH Clinical Center and immediately flash-frozen (<2 minutes from collection) in liquid nitrogen as described (30). All patients gave written informed consent for study inclusion and were enrolled on NCI institutional review board-approved protocols. Study design and conduct complied with all applicable regulations, guidances, and local policies. In addition to needle biopsies, Asterand, Inc. supplied surgically resected large intestine adenocarcinoma tissue from three patients that had been flash-frozen within 20 minutes of excision. Board-certified clinical pathologist review of H&E stained tissue reported tumor content of 50–100% and confirmed the tissue and diagnosis (analysis provided by the supplier).

### Statistical Analysis

Regression analysis and descriptive statistics including mean, standard deviation, standard error of the mean, and coefficient of variation (CV) were conducted with Microsoft Excel 2007 and GraphPad Prism (v5.04). The significance level was set at $\alpha$=0.05 for a two-sided Student’s t-test. Drug-treated xenograft cohorts contained between 4 and 6 animals and were compared to the average biomarker level for vehicle-treated animals collected on the same day of the experiment. Multiplex data were generated by Luminex xPONENT software v3.2, and data analysis was performed using Bio-Plex Manager software v4.0 and higher (Bio-Rad Laboratories) using a five-parametric-curve fitting model for each analyte

independently. To provide an estimate of the biological variation of each biomarker for use when multiple sampling is not possible, the inter-tumor Least Significant Change (LSC) was calculated as described previously ( $LSC = z \times \sqrt[2]{(CV_i)^2 + (CV_a)^2}$ where $CV_i$ is variance in vehicle treated group and $CV_a$ is inter-day analytical variation) (31, 32) using vehicle-treated SW620 and MDA-MB-231 xenograft samples. For comparison, a within-tumor LSC was also calculated from the variance ($CV_i$) between Jurkat xenograft tumor quarters from the same animal. A *z*-value of 1.96 was selected for 95% probability of statistical significance.

## RESULTS

### Assay development and analytical validation

Screening of commercial antibodies in a sandwich immunoassay format against recombinant calibrator proteins was used to select specific capture and detection antibody pairs. To avoid known protein-protein interactions among Bcl-2 family proteins, the multiplex immunoassays were grouped into three panels (1–3) comprised of five target proteins each (Table 1). Specificity for the heterodimeric biomarkers Bax–Bcl-2, Bcl-xL–Bak, and Mcl1–Bak was achieved by using a capture antibody against one binding partner, and then probing using a detection antibody to the interacting protein. The ability to capture and detect these heterodimers was confirmed by immunoprecipitation followed by Western blot using the paired antibodies (Supplemental Fig. S1A–C). Furthermore, Western blotting demonstrated that assay antibodies measure multiple forms of Bim (Bim-EL, Bim-L) and Mcl1 (Mcl1L and Mcl1S), and the lamin-B antibodies detect both intact protein and the 45 kDa cytosolic fragment, the latter of which changed as expected in response to ABT-199 (Supplemental Fig. S1D–F).

Calibrator curves for each panel are shown in Fig. 1A–C. For each assay run, tumor sample lysates were adjusted to 250–500 μg/mL of total protein to allow for detection of antigens with as little as 7.5 μg total protein. Applying LLOQ, F-LOD, and ULOQ criteria, the precision for each biomarker in the assay was <30% CV (details not shown). Inter-assay precision between different operators and instruments on multiple days varied from 4.5% to 26.2% CV (Table 1). Dilution linearity recovery for control lysates diluted 1:2, 1:4, and 1:8 ranged from 59% to 179% (Supplemental Table S1A). Mean recoveries of calibrators spiked into tumor cell or tissue lysates ranged from 46% to 199% (Supplemental Table S1B); recoveries for total lamin-B had the poorest agreement ($r<0.5$) between the two spike concentrations with percent recovery consistently <60%. Overall inter-laboratory agreement between two laboratories determined using three xenograft tumor control lysates was within 8% ± 17% (mean ± SD) (Supplemental Table S2A).

The multiplexing process did not affect the specificity of assays; only Bax showed any signal intensity (approximately 5%) in the tissue lysates when evaluated for Bak as a single analyte versus the mixed analyte samples, indicating that the presence of multiple antibodies in the same well was not detrimental to analyte specificity. Bax and Bak are known to interact in cancer cells; therefore, the cross-reacting signal could be due to the presence of a Bax–Bak heterodimer. The specificity of each individual antibody was confirmed by

immunoprecipitation and immunoblotting, including determination of isoform and post-translational modifications (data not shown).

### Pre-analytical variables

Total tissue lysate samples were stable at 2–8°C for up to 4 hours in all three panels (Supplemental Fig. S2A–C). In contrast, storage at 20–25°C for 24 hours resulted in increased levels of activated caspase-3 presumably linked to mixing activators of caspase-3 released from the mitochondrial/nuclear fraction with cytosolic total caspase-3 (Supplemental Fig. S2C). Thus, samples were stable for the duration of assay sample processing. Up to three freeze thaw cycles had minimal impact (≤20% random error) on analyte concentrations (Supplemental Fig. S3A–C).

The fractionation and cell extraction procedure yielded >500 μg/mL total protein from six different xenograft tumor quadrants with satisfactory fractionation efficiency (<10% contamination) as demonstrated by cytosolic and mitochondrial markers (Fig. 1D). Cytosolic and mitochondrial/nuclear fractions from several untreated tumor xenograft models evaluated with the multiplex immunoassays demonstrated a wide range of baseline biomarker levels (Fig. 2). The fractional distribution of various biomarkers was consistent with known localization, including the previously published absence of any caspase-3 in MCF-7 cells (33). Bak, alone and complexed with Bcl-xL and Mcl1, and lamin-B were primarily detected in the mitochondrial/nuclear fraction. Caspase-3 and the lamin-B degradation products (45 and 67 kD fragments) were primarily detected in the cytosolic fraction (Supplemental Fig. S1F). Other markers were found in both cytosolic and mitochondrial/nuclear fractions.

### Tumor growth inhibition following TL32711 administration

TL32711 significantly inhibited MDA-MB-231 xenograft tumor growth compared to vehicle by the sixth day after the initial dose (Fig. 3). Tumor weights were significantly different from vehicle-treated control for both 4 mg/kg and 12 mg/kg dose groups, but only the 12 mg/kg dose group achieved regression (by 35%, $p<0.001$) relative to starting tumor weight (Fig. 3A). In OVCAR3 xenografts, treatment with TL32711 at 12 mg/kg dose (Fig. 3C) resulted in non-significant ($p=0.077$) changes in tumor weight as compared to control group. Body weight did not change significantly between drug- and vehicle-treated groups over the study period and did not exceed 5% loss in any animal (data not shown).

### Fitness-for-purpose modeling in xenograft models

A dose-dependent activation of intratumoral caspase-3 was detected in MDA-MB-231 xenografts 6 hours after administering the first dose of TL32711, increasing 8.4- and 20.9-fold for the 4 mg/kg and 12 mg/kg dose groups, respectively, over the mean of the paired vehicle-treated group ($P\leq.01$; Fig. 4A). Increased active caspase-3 was accompanied by a dose-dependent 1.8- and 5.1-fold increase in total cytosolic lamin-B at the same time point after the first dose ($P\leq.01$; Fig. 4B). Cytosolic lamin-B is indicative of the execution of apoptosis, because lamin-B only appears in the cytosol as protein fragments following nuclear lamina breakdown. Corresponding significant reductions in the cytosolic levels of the pro-survival protein Bcl-xL were more pronounced at 12 mg/kg than 4 mg/kg ($P\leq.0001$

after dose 1; $P \leq .05$ after dose 3) (Fig. 4C). Increased levels of active caspase-3 positively correlated with increased lamin-B levels in individual mouse samples, indicating that biomarker concentrations followed the expected series of events during apoptosis pathway activation (Supplemental Fig. S4). Levels of other biomarkers were not significantly changed after treatment (data not shown). In the non-responsive OVCAR3 model (25), TL32711 treatment increased cytosolic cleaved caspase-3 levels by only 45% at most (Fig. 4D), and the only significant changes in cytosolic Lamin-B levels were modest decreases ($P \leq .05$) (Fig. 4E). Significant decreases in cytosolic Bcl-xL levels were observed after the third dose of TL32711, though the magnitude was smaller than in MDA-MB-231 (20% to 42%; $P \leq .05$) (Fig. 4F).

## Modeling clinical sample collection, longitudinal sampling, and biological variability

When using longitudinal sampling to evaluate biomarker levels (e.g., pre- and post-treatment biopsies), multiple sampling to measure inherent biomarker variability is not possible, so knowledge of the normal biological variability (i.e., the "sampling variability") of the biomarker at baseline is needed to attribute changes to drug effect rather than random variability. In addition, estimates of biological variability are required to establish the normal range of biomarker levels expected in the clinic. We simulated this in breast (MDA-MB-231) and colon cancer (SW620) xenograft models by combining the inter-tumor variance measured from all the individuals in the vehicle-treated groups with the analytical variance of the assay to calculate the LSC needed to be considered drug-induced in serial patient measurements. The LSC was between 31% and 128% for each of the 15 biomarkers in this assay, but varied by xenograft model and cellular fraction (Supplemental Table S2B). For comparison, we also determined the within-tumor variability by measuring each biomarker in all four quadrants of Jurkat xenografts. The average within-tumor variability of the biomarkers was 9% to 31%, corresponding to within-tumor LSC values of 24% to 66% (Supplemental Table S3). In the context of biomarker measurements in serial biopsies, the larger variability estimates calculated from inter-tumoral sampling appear to be more appropriate.

## Establishing clinical readiness in human tumor needle biopsy samples

Four 18-gauge core needle biopsies (two from the liver of a patient with esophageal cancer, one from the supraclavicular node of a patient with an unknown primary cancer, and one from the liver of a patient with colon cancer) were processed into fractionated cell lysates. Protein concentrations were 860–970 μg/mL and 230–510 μg/mL for the cytosolic and mitochondrial/nuclear fractions, respectively. The multiplex immunoassays were able to quantify baseline levels of each biomarker assayed from at least one biopsy, with the exception of Bax–Bcl-2 (Fig. 5). Bak, lamin-B, Bim, Mcl1–Bak, survivin, and pS99-Bad were only measurable in a subset of samples; some values for total caspase-3 and total lamin-B were above the assay ULOQ but would be measurable after sample dilution. Of the 15 biomarkers measured from 4 biopsies, 82% of all analytes in the mitochondrial/nuclear fractions, and 65% of all analytes in the cytosolic fractions were quantifiable (>LLOQ). Of these, 80% of mitochondrial/nuclear levels and 59% of cytosolic levels allowed for drug-induced decreases in the biomarker, as defined by the LSC, within the assay's dynamic

range. All drug-induced biomarker increases should be measurable after sufficient sample dilution.

## DISCUSSION

Aberrant expression of anti-apoptotic proteins such as Bcl-2 or the suppression of pro-apoptotic members such as Bax or Smac can lead to tumor formation and promote resistance to therapy in many types of cancer by delaying or blocking the normal execution of apoptosis. Currently, it is believed that initiation of apoptosis does not require transcription or translation of new proteins; rather, apoptotic signals trigger changes in normally dormant proteins including post-translational modifications and protein-protein and protein-membrane interactions to initiate cell death. In this study we applied a multi-marker immunoassay approach to study the modulation of an array of proteins with established relevance to extrinsic and intrinsic apoptotic pathways in response to TL32711 treatment. Biomarker selection was based on availability of specific antibodies, purified recombinant proteins, and the feasibility of measurement in an immunoassay format; therefore, assays for some potentially informative complexes, such as larger multimers or homodimers, were not developed. Recent advances in multiplexed sandwich immunoassays allowed us to design an assay to detect both monomeric and heterodimeric forms of Bcl-2 family proteins to measure neutralization of anti-apoptotic (Bcl-2, Bcl-xL, Mcl1) or release of pro-apoptotic (Bax and Bak) proteins. Assessing the oligomeric state of Bcl-2 family members rather than their absolute levels represents a novel approach in quantitative apoptosis profiling. Because sampling times in the clinic vary widely, the assays were designed to quantify both early apoptotic events, e.g., active (cleaved) caspase-3 (17 kD fragment), and later effects, such as cytosolic lamin-B fragments known to be generated by active caspase-3 during nuclear lamina breakdown (34). Including both early and later biomarkers of drug action should increase the likelihood of detecting an apoptotic signal across clinical trials of multiple agents. The advantages offered by multiplex analysis make it useful in clinical trials where only limited samples are available for PD measurements. The need to fractionate cell lysates to achieve functional specificity may limit how many of the multiplex panels can be used to assay material from a single 18-gauge needle biopsy; limited protein yields may also require prioritization of the panels based on intended drug mechanism of action. Our clinical modeling indicates that absolute protein concentrations per volume rather than total protein yields, per se, were limiting factors for all three panels. Generating a total cell lysate might yield higher protein concentrations than fractionated cell lysates, but is not recommended because, as our stability data show, this can trigger artificial caspase-3 activation.

The validated multiplex immunoassays described herein exhibited robust sensitivity, specificity, and reproducibility using tumor xenografts of human cancer cell lines. As expected, tumor cell lines demonstrated variable biomarker levels; the subcellular distribution of the majority of markers was consistent with previous reports (17, 24, 33). The sensitivity of the assay was adequate to detect levels of the majority of apoptotic proteins in at least one of the six tumor xenograft models under test conditions. Low Bim levels are often caused by reduced message stability and proteasome-dependent turnover (35), but our assay reliably detected baseline levels of Bim in xenografts (LLOQ 0.046 ng/mL). Assay

specificity within each panel was excellent; measurement of any protein in the multiplexed format did not interfere with measurement of any other protein.

Analytical validation revealed some anomalies such as low dilution and spike recoveries for total lamin-B in every tumor lysate analyzed. Potential explanations for this include: 1) proteolytic degradation, a common biochemical feature of apoptosis that could result in undetectable protein fragments smaller than 45 kDa; 2) oligimerization that could prevent antibody binding; and 3) potential interactions with the nuclear lamina that could influence its solubility and thus recovery. Therefore, although lamin-B had low spike recoveries (46%–57%), there is adequate justification to retain this biomarker as long as sample recovery is taken into consideration when interpreting clinical data. The validated assay exhibited robust accuracy for many of the PD biomarkers; however, levels of lamin-B, Bcl-xL–Bak, survivin, Mcl1, and Bim fell outside the acceptable recovery range (100% ± 30%) using extracts of some xenografts. Higher expression of proteins that interact with the Bcl-2 family may interfere in the assay by altering the equilibrium of binding partners (Bak–Bim or Bcl-xL–Bim). In general, these observations reflect a spike recovery artifact unique to the analysis of proteins that are in dynamic equilibrium in individual tumor samples rather than poor accuracy. Longitudinal comparison of baseline to post-treatment should minimize the impact of interfering substrates on tumor biomarker quantitation.

MDA-MB-231 and OVCAR3 xenografts treated with the Smac mimetic TL32711 and sampled at time points relevant for clinical protocols established the fitness of the assay for measuring appropriate biomarkers of apoptosis. TL32711 primarily targets IAPs, suppression of which results in activation of caspases; clinically relevant doses of TL32711 in the responsive MDA-MB-231 model caused up to 21-fold activation of cytosolic caspase-3 within 6 hours and coincided with significant increases in cytosolic lamin-B (intact and 45 kDa fragment), indicating the breakdown of nuclear lamina and the execution of apoptosis (34). Significant reductions in Bcl-xL levels were observed 6 to 24 hours after TL32711 treatment. Previous studies have demonstrated cleavage of Bcl-xL and Bcl-2 by caspase-3, which removes the anti-apoptotic BH4 domain and transforms them into pro-apoptotic proteins resembling Bax and Bak (36, 37). The sequence of caspase-3 activation within 6 hours of TL32711 treatment followed by decreased Bcl-xL levels after 24 hours is consistent with this mechanism, and demonstrates fitness-for-purpose of the multiplex immunoassays in measuring primary (active caspase-3) and secondary (lamin-B and Bcl-xL) PD endpoints. The modulation of these biomarkers was dose-dependent and also correlated with therapeutic effect (decreased tumor volume), including in the non-responsive OVCAR3 xenograft model, which displayed minimal changes in active caspase-3 and lamin-B levels. Together, these preclinical models clearly demonstrated that biomarker modulation correlated with anti-tumor efficacy.

Clinical readiness of the validated assay was demonstrated by evaluating solid tumors of different histologies from three untreated patients. Of the 15 PD biomarkers, all but Bax–Bcl-2 were quantified in at least one biopsy fraction, although 5 others (Bak, Bim, Mcl1–Bak, survivin, and pS99-Bad) were quantifiable in only a subset of the clinical specimens. A prerequisite for clinical evaluation of drug action on a target protein is measuring the inherent heterogeneity of protein levels at baseline so that biologic variations and drug-

induced changes can be distinguished; however, parallel sampling is rarely practical or feasible in the clinic, and our LSC results provide some estimates of this variability. While the biological variability for some biomarkers may appear to be too large to be of practical value, two-thirds of all biomarker levels in the mitochondrial/nuclear fractions of the patient samples were high enough to observe an LSC-defined drug-induced decrease within the assay dynamic range. Additionally, up to 21-fold induction of active caspase-3 was measured after TL32711 administration, so relative changes in biomarkers may be several fold higher than total variability when an optimal sampling time is utilized.

In conclusion, we describe validated multiplex immunoassays for evaluating 15 mechanistic biomarkers likely involved in the PD response to drugs targeting apoptosis; this approach demonstrated utility for confirming the proof-of-mechanism of the Smac mimetic TL32711 in vivo. Determining the most useful of these 15 PD biomarkers for a given clinical application will depend on drug mechanism of action and clinical trial design, including biopsy timing. Assay sensitivity and dynamic range are suitable for use in early phase trials profiling apoptotic response and evaluating the mechanism of action of novel compounds targeting the apoptotic pathway. These multiplex apoptosis immunoassays therefore allow a more detailed interrogation of targeted agent activity in tumor biopsies, possibly guiding the timing, dose, and choice of agents for single or combination therapies that induce cancer cell death via modulation of pro-survival and pro-apoptosis proteins.

## Supplementary Material

Refer to Web version on PubMed Central for supplementary material.

## Acknowledgments

The authors recognize and remember the assistance of our colleague on this project, Thomas Jakubowski, who succumbed to GIST during the course of this work. We thank Dr. Larry Rubinstein for help with statistical considerations and Drs. Yvonne A. Evrard and Andrea Regier Voth, Leidos Biomedical Research, Inc., for medical writing support in the preparation of this manuscript.

**Research Support**

This project has been funded in whole or in part with federal funds from the National Cancer Institute, National Institutes of Health, under Contract No. HHSN261200800001E. The content of this publication does not necessarily reflect the views or policies of the Department of Health and Human Services, nor does mention of trade names, commercial products, or organizations imply endorsement by the U.S. Government. This research was supported [in part] by American Recovery and Reinvestment Act funds. There are no other directly related manuscripts, published or unpublished, by any authors of this paper.

## References

1. Hanahan D, Weinberg RA. Hallmarks of cancer: the next generation. Cell. 2011; 144:646–74. [PubMed: 21376230]
2. Fulda S. Evasion of apoptosis as a cellular stress response in cancer. Int J Cell Biol. 2010; 2010:370835. [PubMed: 20182539]
3. Cragg MS, Harris C, Strasser A, Scott CL. Unleashing the power of inhibitors of oncogenic kinases through BH3 mimetics. Nat Rev Cancer. 2009; 9:321–6. [PubMed: 19343035]
4. Sale MJ, Cook SJ. The BH3 mimetic ABT-263 synergizes with the MEK1/2 inhibitor selumetinib/AZD6244 to promote BIM-dependent tumour cell death and inhibit acquired resistance. Biochem J. 2013; 450:285–94. [PubMed: 23234544]

5. Krepler C, Chunduru SK, Halloran MB, He X, Xiao M, Vultur A, et al. The novel SMAC mimetic birinapant exhibits potent activity against human melanoma cells. Clin Cancer Res. 2013; 19:1784–94. [PubMed: 23403634]
6. Corcoran RB, Cheng KA, Hata AN, Faber AC, Ebi H, Coffee EM, et al. Synthetic lethal interaction of combined BCL-XL and MEK inhibition promotes tumor regressions in KRAS mutant cancer models. Cancer Cell. 2013; 23:121–8. [PubMed: 23245996]
7. Allensworth JL, Sauer SJ, Lyerly HK, Morse MA, Devi GR. Smac mimetic Birinapant induces apoptosis and enhances TRAIL potency in inflammatory breast cancer cells in an IAP-dependent and TNF-alpha-independent mechanism. Breast Cancer Res Treat. 2013; 137:359–71. [PubMed: 23225169]
8. Fulda S, Vucic D. Targeting IAP proteins for therapeutic intervention in cancer. Nat Rev Drug Discov. 2012; 11:109–24. [PubMed: 22293567]
9. Nakahara T, Kita A, Yamanaka K, Mori M, Amino N, Takeuchi M, et al. YM155, a novel small-molecule survivin suppressant, induces regression of established human hormone-refractory prostate tumor xenografts. Cancer Res. 2007; 67:8014–21. [PubMed: 17804712]
10. Pan Y, Xu R, Peach M, Huang CP, Branstetter D, Novotny W, et al. Evaluation of pharmacodynamic biomarkers in a Phase 1a trial of dulanermin (rhApo2L/TRAIL) in patients with advanced tumours. Br J Cancer. 2011; 105:1830–8. [PubMed: 22033270]
11. Hector S, Prehn JH. Apoptosis signaling proteins as prognostic biomarkers in colorectal cancer: a review. Biochim Biophys Acta. 2009; 1795:117–29. [PubMed: 19167459]
12. Stearns V, Jacobs LK, Fackler M, Tsangaris TN, Rudek MA, Higgins M, et al. Biomarker modulation following short-term vorinostat in women with newly diagnosed primary breast cancer. Clin Cancer Res. 2013; 19:4008–16. [PubMed: 23719261]
13. Ward TH, Cummings J, Dean E, Greystoke A, Hou JM, Backen A, et al. Biomarkers of apoptosis. Br J Cancer. 2008; 99:841–6. [PubMed: 19238626]
14. Dean E, Greystoke A, Ranson M, Dive C. Biomarkers of cell death applicable to early clinical trials. Exp Cell Res. 2012; 318:1252–9. [PubMed: 22483936]
15. Cotter TG. Apoptosis and cancer: the genesis of a research field. Nat Rev Cancer. 2009; 9:501–7. [PubMed: 19550425]
16. Fulda S, Debatin KM. Extrinsic versus intrinsic apoptosis pathways in anticancer chemotherapy. Oncogene. 2006; 25:4798–811. [PubMed: 16892092]
17. Schinzel A, Kaufmann T, Borner C. Bcl-2 family members: integrators of survival and death signals in physiology and pathology [corrected]. Biochim Biophys Acta. 2004; 1644:95–105. [PubMed: 14996494]
18. Llambi F, Moldoveanu T, Tait SW, Bouchier-Hayes L, Temirov J, McCormick LL, et al. A unified model of mammalian BCL-2 protein family interactions at the mitochondria. Mol Cell. 2011; 44:517–31. [PubMed: 22036586]
19. Guerrero AD, Schmitz I, Chen M, Wang J. Promotion of Caspase Activation by Caspase-9-mediated Feedback Amplification of Mitochondrial Damage. J Clin Cell Immunol. 2012; 3:1000126. [PubMed: 23539542]
20. Walensky LD. From mitochondrial biology to magic bullet: navitoclax disarms BCL-2 in chronic lymphocytic leukemia. J Clin Oncol. 2012; 30:554–7. [PubMed: 22184389]
21. Fulda S. Molecular pathways: targeting inhibitor of apoptosis proteins in cancer--from molecular mechanism to therapeutic application. Clin Cancer Res. 2014; 20:289–95. [PubMed: 24270683]
22. Green DR, Chipuk JE. Apoptosis: Stabbed in the BAX. Nature. 2008; 455:1047–9. [PubMed: 18948940]
23. Westphal D, Dewson G, Czabotar PE, Kluck RM. Molecular biology of Bax and Bak activation and action. Biochim Biophys Acta. 2011; 1813:521–31. [PubMed: 21195116]
24. Youle RJ, Strasser A. The BCL-2 protein family: opposing activities that mediate cell death. Nat Rev Mol Cell Biol. 2008; 9:47–59. [PubMed: 18097445]
25. Benetatos CA, Mitsuuchi Y, Burns JM, Neiman EM, Condon SM, Yu G, et al. Birinapant (TL32711), a bivalent SMAC mimetic, targets TRAF2-associated cIAPs, abrogates TNF-induced NF-kappaB activation, and is active in patient-derived xenograft models. Mol Cancer Ther. 2014; 13:867–79. [PubMed: 24563541]

26. Condon SM, Mitsuuchi Y, Deng Y, Laporte MG, Rippin SR, Haimowitz T, et al. Birinapant, a smac-mimetic with improved tolerability for the treatment of solid tumors and hematological malignancies. J Med Chem. 2014; 57:3666–77. [PubMed: 24684347]
27. Bunch KP, Noonan AM, Lee J-m, O'Sullivan CCM, Houston ND, Ekwede I, et al. Pharmacodynamic biomarkers from phase II study of the SMAC (Second Mitochondrial-Derived Activator of Caspases)-mimetic birinapant (TL32711; NSC 756502) in relapsed platinum-resistant epithelial ovarian cancer (EOC), primary peritoneal cancer (PPC), or fallopian tube cancer (FTC) (NCT01681368). J Clin Oncol. 2014; 32(suppl):abstr 5585.
28. Plowman, J.; Dykes, D.; Hollingshead, M.; Simpson-Herren, L.; Alley, M. Human tumor xenograft models in NCI drug development. In: Teicher, B., editor. Anticancer drug development guide Preclinical screening, clinical trials, and approval. Totowa, NJ: Humana Press Inc; 1997. p. 101-25.
29. Kinders RJ, Hollingshead M, Khin S, Rubinstein L, Tomaszewski JE, Doroshow JH, et al. Preclinical modeling of a phase 0 clinical trial: qualification of a pharmacodynamic assay of poly (ADP-ribose) polymerase in tumor biopsies of mouse xenografts. Clin Cancer Res. 2008; 14:6877–85. [PubMed: 18980982]
30. DCTD Research Resources: Tumor Frozen Needle Biopsy Specimen Collection and Handling. [cited 2014 March 10]; Available from: http://dctd.cancer.gov/ResearchResources/biomarkers/docs/par/SOP340507_Biopsy_Frozen.pdf
31. Sebastian-Gambaro MA, Liron-Hernandez FJ, Fuentes-Arderiu X. Intra- and inter-individual biological variability data bank. Eur J Clin Chem Clin Biochem. 1997; 35:845–52. [PubMed: 9426342]
32. Fraser CG, Harris EK. Generation and application of data on biological variation in clinical chemistry. Crit Rev Clin Lab Sci. 1989; 27:409–37. [PubMed: 2679660]
33. Janicke RU, Sprengart ML, Wati MR, Porter AG. Caspase-3 is required for DNA fragmentation and morphological changes associated with apoptosis. J Biol Chem. 1998; 273:9357–60. [PubMed: 9545256]
34. Shimizu T, Cao CX, Shao RG, Pommier Y. Lamin B phosphorylation by protein kinase calpha and proteolysis during apoptosis in human leukemia HL60 cells. J Biol Chem. 1998; 273:8669–74. [PubMed: 9535842]
35. Ewings KE, Wiggins CM, Cook SJ. Bim and the pro-survival Bcl-2 proteins: opposites attract, ERK repels. Cell Cycle. 2007; 6:2236–40. [PubMed: 17881896]
36. Clem RJ, Cheng EH, Karp CL, Kirsch DG, Ueno K, Takahashi A, et al. Modulation of cell death by Bcl-XL through caspase interaction. Proc Natl Acad Sci U S A. 1998; 95:554–9. [PubMed: 9435230]
37. Cheng EH, Kirsch DG, Clem RJ, Ravi R, Kastan MB, Bedi A, et al. Conversion of Bcl-2 to a Bax-like death effector by caspases. Science. 1997; 278:1966–8. [PubMed: 9395403]

## Translational Relevance

Evaluation of the pharmacodynamic effects/mechanisms of action of the many investigational pro-apoptosis agents currently undergoing clinical investigation has been hindered by the absence of validated biomarker assays capable of providing quantitative measurements of drug effect in the tumor. We therefore developed novel multiplex immunoassays to measure 15 critical biomarkers of apoptosis induction and suppression applicable to needle biopsies of human tumors in the clinic. The use of this validated assay in clinical trials of novel pro-apoptotic agents will allow direct and quantitative profiling of drug effects in tumor target tissues, including evaluation of transient, heterodimeric protein complexes that regulate the suppression and induction of apoptosis. We anticipate that assay results will promote greater understanding of pharmacodynamic modulation that will inform clinical decisions about dose levels, treatment schedules, and combination therapies for this promising class of drugs.

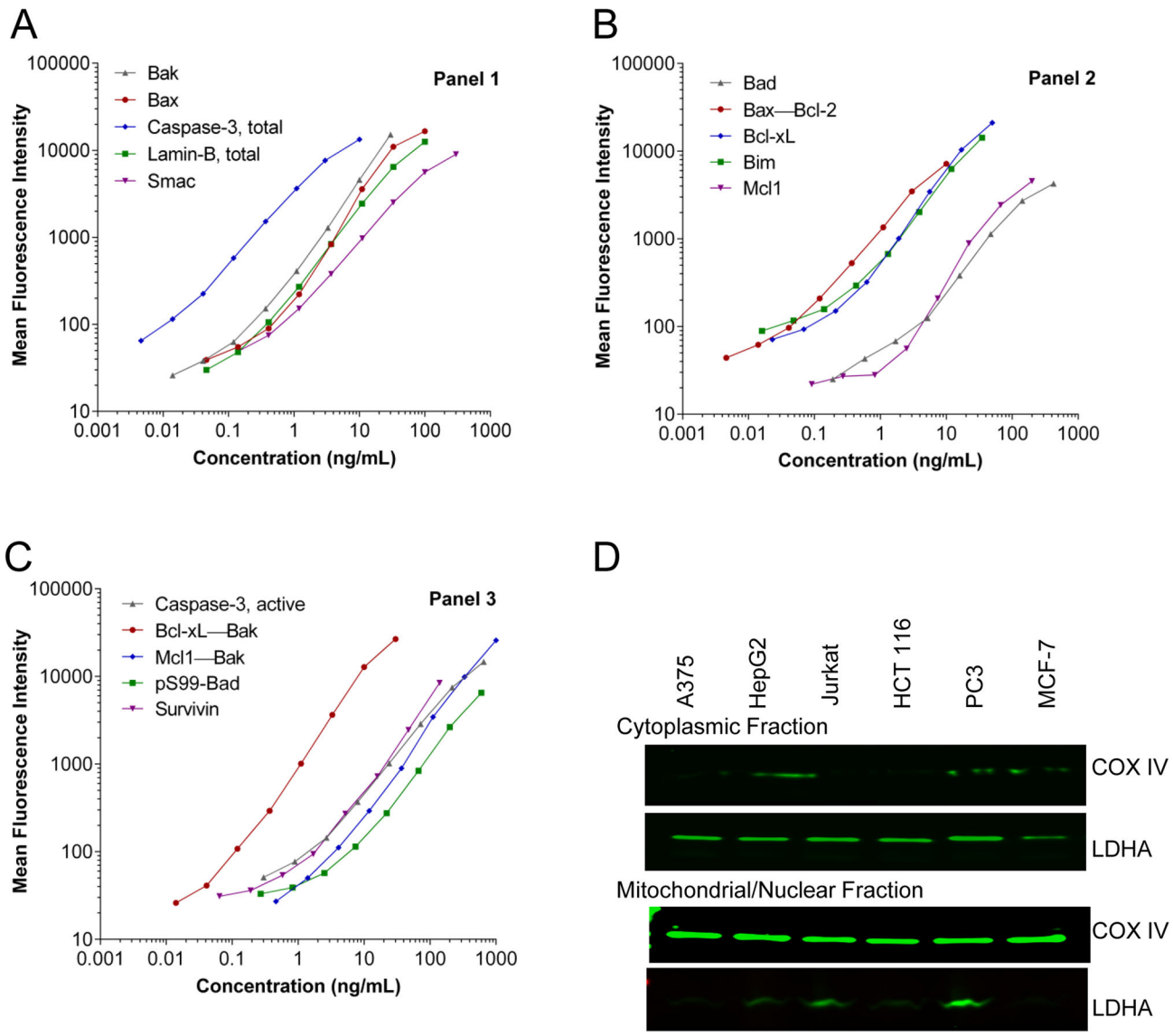


**Figure 1. Validation of the apoptosis multiplex immunoassay panels 1, 2, and 3**

(**A–C**) Calibration curves for three five-plex panels using recombinant protein calibrators to demonstrate the dynamic range of the assays. Data were analyzed using a five-parametric regression formula and plotted on log–log axis (n≥50 beads/data point). (**D**) Tumor lysates generated from six different xenografts were fractionated and analyzed for the efficiency of fractionation using cytosolic (LDHA) and mitochondrial (COX IV) markers.

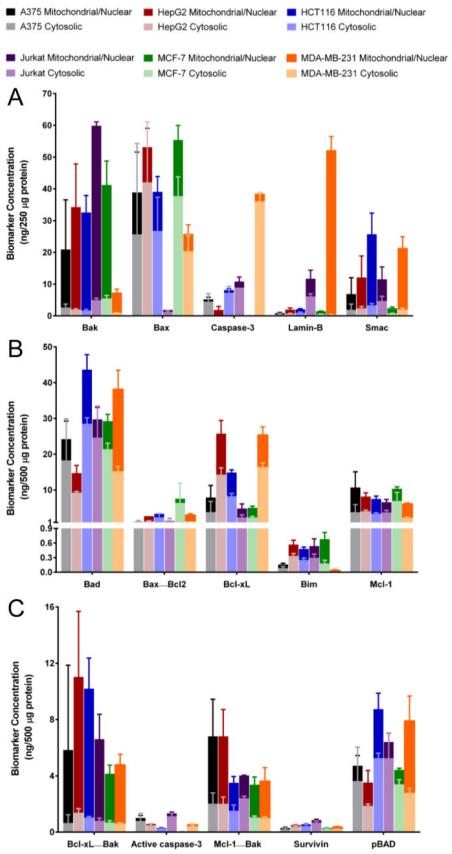


**Figure 2. Analysis of baseline levels of apoptosis biomarkers in select xenograft models using multiplex immunoassay panels 1, 2, and 3**

Cytosolic and mitochondrial/nuclear fractions of tumor lysates from MDA-MB-231 (breast adenocarcinoma), A375 (melanoma), HCT 116 (colorectal carcinoma), HepG2 (hepatocellular carcinoma), Jurkat (T-cell leukemia), and MCF-7 (breast adenocarcinoma) xenografts were analyzed by (**A**) panel 1, (**B**) panel 2, and (**C**) panel 3 of the multiplex immunoassays using 30 µL samples of 500 µg/mL total protein. Error bars are mean ± SD, n = 4 (tumor quadrants from four mice) with mitochondrial/nuclear levels stacked above cytosolic levels. Some lysates did not contain detectable signals, such as the known absence of detectable total and active (cleaved) caspase-3 in MCF-7 xenograft extracts (33).

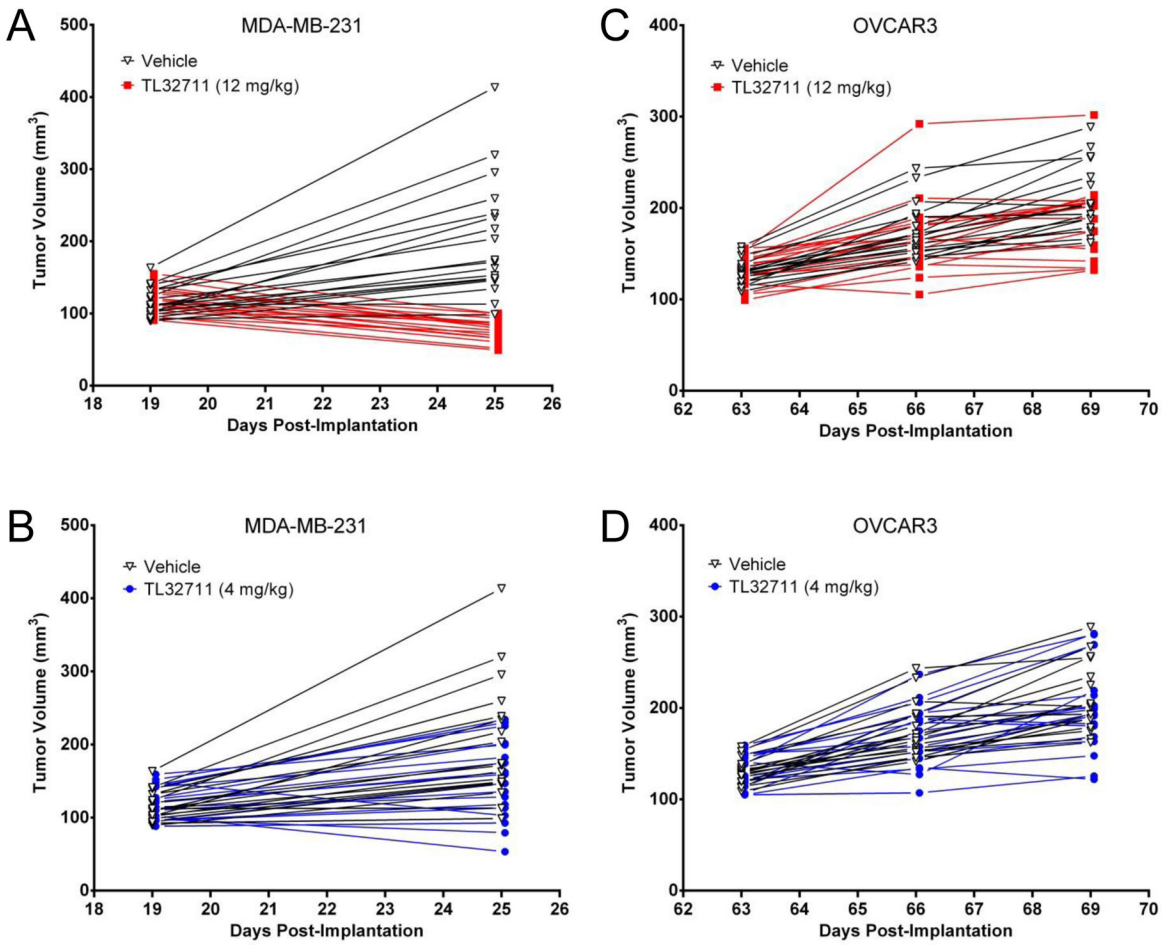


**Figure 3. Anti-tumor efficacy of TL32711 against MDA-MB-231 and OVCAR3 xenografts**

**(A, B)** MDA-MB-231 xenografts were treated with TL32711 on days 19, 22, and 25 post-implantation, and **(C, D)** OVCAR3 xenografts were treated on days 63, 66, and 69 post-implantation due to slower tumor growth. The individual progression of each animal is plotted.

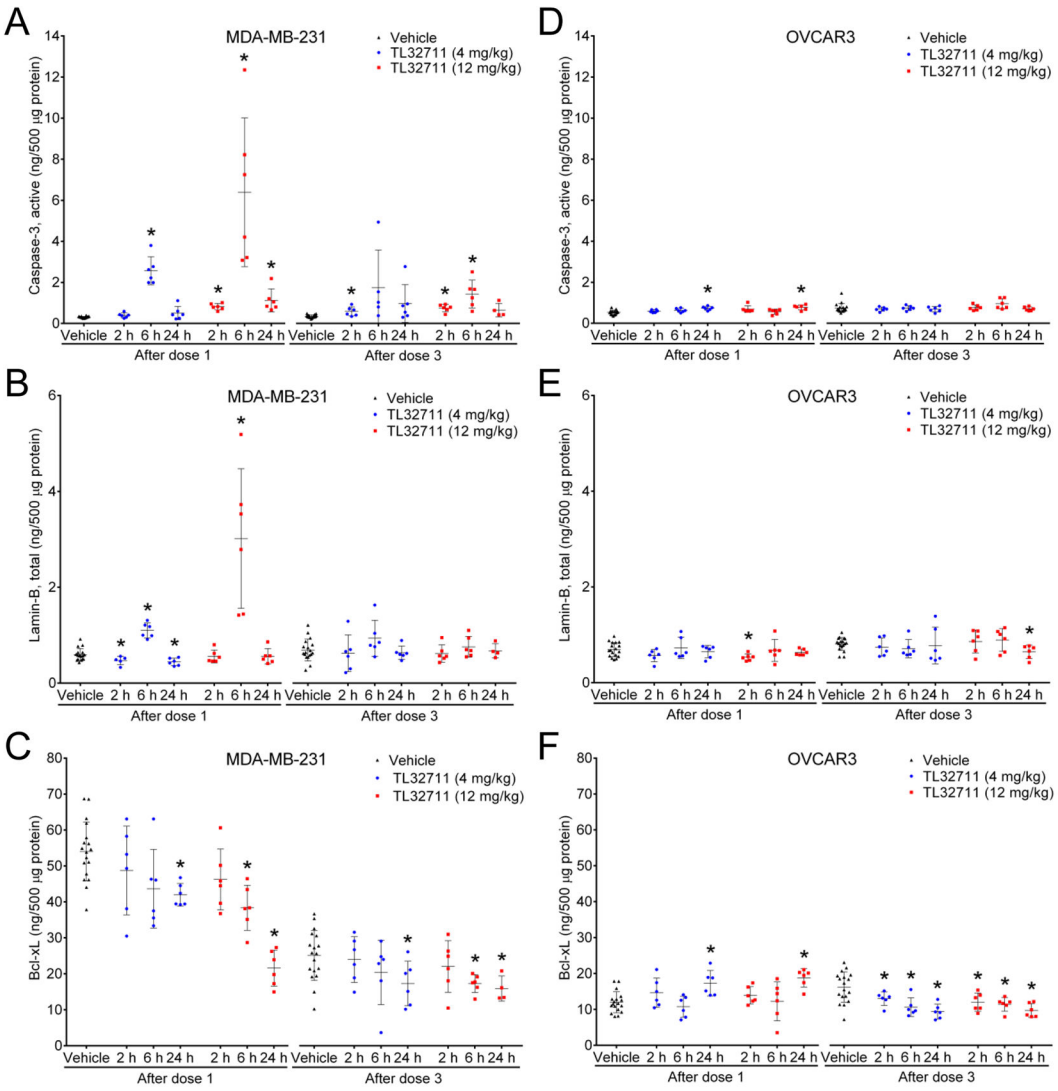


**Figure 4. The effect of TL32711 on active caspase-3, total lamin-B, and Bcl-xL in MDA-MB-231 and OVCAR3 xenografts**

Xenograft quarters collected at the indicated time intervals after drug or vehicle treatment were analyzed using the multiplex immunoassays, and changes in cytosolic (**A, D**) active (cleaved) caspase-3, (**B, E**) total lamin-B, and (**C, F**) Bcl-xL levels compared to grouped vehicle-treated controls from the same day. Error bars, mean ± SD; asterisks, $P \leq .05$ for the group comparison.

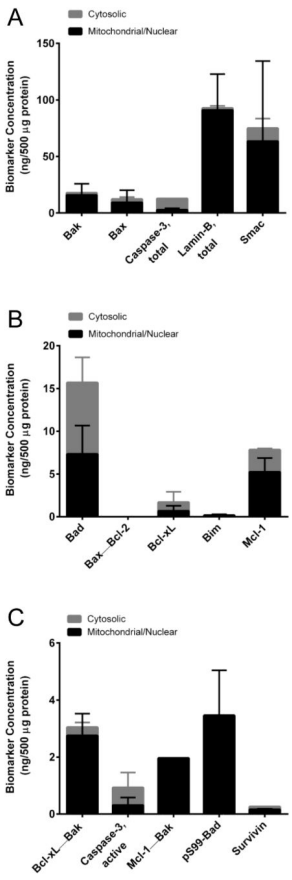


**Figure 5. Survey of apoptosis biomarkers in needle biopsies from patients**

Four 18-gauge tumor needle biopsies from 3 patients with solid tumors (one with esophageal cancer, one with an unknown primary cancer, and one with colon cancer) were fractionated and cytosolic and mitochondrial/nuclear fractions were analyzed by (**A**) panel 1, (**B**) panel 2, and (**C**) panel 3 of the multiplex immunoassays using 30 µL samples of 500 µg/mL total protein. Individual analyte measurements below LLOQ were not included in the group average (for example, some Bak, Bim, Mcl1–Bak, survivin, and pS99-Bad values, and all Bax–Bcl-2 values), while measurements above ULOQ were included as the ULOQ (for example, some lamin-B and total caspase-3 values). Error bars, mean ± SD.

**Table 1**

Analytical sensitivity and reproducibility of multiplex immunoassays

| | | | Analyte Levels, Mean ± SD (ng/500 μg total protein) | | | Inter-assay %CV | | |
|---|---|---|---|---|---|---|---|---|
| **Multiplex Panel #** | **Analyte** | **Sensitivity (LLOQ) ng/mL** | **Low Control** | **Mid Control** | **High Control** | **Low Control** | **Mid Control** | **High Control** |
| Panel 1 | Bak | 0.78 | 1.97±0.38 | 7.93±1.21 | 101±6 | 19.5 | 15.3 | 5.7 |
| | Bax | 0.89 | 3.05±0.38 | 19.08±3.57 | 105±14 | 25.5 | 18.7 | 13.4 |
| | Caspase-3, total | 0.0073 | 0.017±0.004 | 0.52±0.07 | 3.02±0.34 | 23 | 14.3 | 11.2 |
| | Lamin-B, total | 0.14 | 0.84±0.16 | 5.55±1.16 | 22±3 | 19.5 | 20.9 | 12.6 |
| | Smac | 0.5 | 1.09±0.29 | 10.36±1.42 | 86±15 | 26.2 | 13.7 | 16.8 |
| Panel 2 | Bad | 0.52 | 2.40±0.32 | 28±3 | 39±2 | 13.2 | 9.5 | 4.9 |
| | Bax–Bcl-2 | 1.9 | 9.65±1.67 | 97±12 | 370±36 | 17.3 | 11.9 | 9.9 |
| | Bcl-xL | 0.089 | 0.28±0.07 | 4.8±0.22 | 25±1.18 | 25.1 | 4.5 | 4.7 |
| | Bim | 0.046 | 0.16±0.02 | 1.01±0.13 | 7.82±1.03 | 12.4 | 13.1 | 13.1 |
| | Mcl1 | 1.2 | 2.24±0.23 | 10.9±0.54 | 54±4 | 10.5 | 5 | 6.9 |
| Panel 3 | Bcl-xL–Bak | 0.11 | 0.68±0.10 | 5.49±0.64 | 23±2 | 14.3 | 11.7 | 10.4 |
| | Caspase-3, active | 0.062 | 0.34±0.05 | 2.39±0.24 | 9.7±0.65 | 13.2 | 9.9 | 6.7 |
| | Mcl1–Bak | 1.2 | 21.95±2.41 | 100±8 | 402±37 | 11 | 8 | 9.1 |
| | pS99-Bad | 2.1 | 4.55±0.69 | 17±2.06 | 137±8 | 15.2 | 12.2 | 6.2 |
| | Survivin | 0.11 | 1.59±0.20 | 4.73±0.58 | 19±1.76 | 12.4 | 12.2 | 9.3 |

Abbreviations: CV, coefficient of variation; SD, standard deviation; LLOQ, lower limit of quantitation (mean + 10 × SD of blank signal, n=20)